CHAPTER 1

Introduction

1.1 Statement and Significance of the Problem

The bone matrix is precisely composed of two major phases at the nanoscale level namely, organic (cells, proteins, lipids, *etc*.) and inorganic (minerals); and may be considered as a good example for a nanocomposite. These phases have multiple components which consist of, in decreasing proportions, minerals, collagen, water, non-collagenous proteins, lipids, vascular tissue elements, and cells [1-3]. The bone mineral is mainly composed of calcium phosphate and the bone protein is mainly composed of collagen. Collagen is a structural fiber in form plate-like tiny crystals of calcium phosphate are inlayer to strengthen the bone [4]. Collagen has a typical fibrous structure, whose diameter varies from 100 to 2000 nm. Similarly, calcium phosphate in the bone mineral is in the form of nanocrystals, with dimensions of about 4 nm by 50 nm by 50 nm [5, 6].

Calcium phosphate such as hydroxyapatite (HA), β-tricalcium phosphate (β-TCP) and biphasic calcium phosphate (BCP), have been largely used as bone grafts for bone replacement, proliferation or substitution. The necessity of bone grafts depends on the complexity of the bone defects. For instance, if the defect is minor, bone has its own potential to self remodeling within a few weeks. Therefore, surgery is not required. But in another case of violent defects and loss of volume, bone could not heal by itself and grafting is required to restore integrity without damaging living tissues. There are multiple methods available for the treatment of bone defects, which includes the traditional methods of autografting, allografting and xenografting. Even if autografting and allografting are clinically considered as good therapies, they have limitations. For instance, supply of autograft is limited and there is a possibility of disease transmission from allograft. Accordingly, there is a great need for the use of

synthetic bone grafts. Nowadays, numerous synthetic bone graft materials, both single and multiphase are available which are capable of moderate some of the practical complications associated with the autogenous, allogeneic or xenogenic bones. Although there is good progress in bone grafting using synthetic bone grafts, the way in which they execute their functions in vivo is quite different and most of them differ from natural bone either composition or structure [7-9].

With statistical reports from worldwide, In the United States of America (USA), there are an estimated 280,000 hip fractures, 700,000 vertebral, and 250,000 wrist fractures of patients each year at a cost of $10 billion [10]. Delayed healing or nonunion occurs in 5 per cent of all fractures, and 20 per cent of high impact fractures [11]. Large areas of bone loss due to trauma may exceed the body's regenerative capabilities unless surgeons intervene to bridge the skeletal defect. Management of a non-union is a challenging and costly exercise, and provides a target for further bone tissue engineering strategies. The demand in the surgical market is highlighted by the fact there are around 4,000,000 operations involving bone grafting or bone substitutes performed around the world annually [12]. In Europe, the number of bone grafting procedures was reported to be 287,300 in 2000 and it is expected that it could be increased to about 479,079 in 2005 [13]. In Thailand, the demand for medical equipment has increased annually. According to the forecasts of department of business economics Thailand, Ministry of commerce, the growth rate of demand increased estimately 9.1 percent per year.

For instance, in 2010, Thailand has imported medical equipment increasingly from 25,928 million baths to about 38,000 million baths by the year 2014. Every year, Thailand has imported medical equipment over exported deficit of 5,000 million yearly and it is expected to trend deficit increased. For bone graft, Thailand has imported from abroad nearly 100 percents. Mostly, Thailand has imported medical device and equipment in classified of medium technology and high technology from the USA, Japan and Singapore. Therefore, bone graft materials have expensively affected to patients who are poor. The patient could not be treated as valid and appropriate. Moreover, some medical devices had been designed for foreigners only,

so that it is not appropriate for anatomy of Asian people. Therefore, it makes use of some obstacles and effective in the treatment of patients decreased [14].

1.2 Literature Review

Yeong *et al.* [15] synthesized HA using a mechanochemical method from calcium oxide (CaO) and anhydrous calcium hydrogen phosphate ($CaHPO_4$). A singe phase HA of high crystallinity was achieved by increasing 20 h of activation time without further thermal treatment at high temperatures. The resulting HA powder exhibits an average particle size of approximately 25 nm and a specific surface area 76.06 m^2/g, measured by the multipoint Brunauer–Emmett–Teller (BET) technique. It was sintered to a density of 98.20% theoretical density at 1200°C, for 2 h.

Abdeslam *et al*. [16] investigated the influence of adding water to the kinetics of a mechanochemical reaction of dicalcium phosphate dihydrate (DCPD) with calcium oxide (CaO). The DCPD disappearance rate, constant k, and the final reaction, time t_f, were determined in each case and correlated with the water content present in the slurry. Results showed that the addition water (1) slowed down the reaction rate, (2) increased the powder contamination by the milling material (hard porcelain) due to ball and vial erosion; and that (3) wet milling did not generate the expected products, in contrast to dry grinding, because porcelain induced HA decomposition with the formation of beta-tricalcium phosphate (β-TCP) and silicon stabilized TCP. Consequently, dry mechanosynthesis appears preferable to wet milling in the preparation of calcium phosphates for biological interest.

Guo *et al*. [17] prepared pure tetracalcium phosphate (TTCP) powder through a solid state phase reaction, at 1500°C. The effects of cool down modes on the synthesizing process of TTCP powder and its thermal behavior at different heating temperatures were investigated by X-Ray Diffraction (XRD) and Fourier Transform Infrared Spectroscopy (FTIR). The results showed that cooling in dry air tends to promote the formation of single phase TTCP, while in situ cooling in a furnace results in a mixture of HA and CaO. The examination of the thermal behavior of TTCP

indicates that a decomposing zone exists in the high temperature range of 500°C – 1200°C. TTCP phase is transformed during the subsequent cooling process. This was confirmed by three additional cooling treatment routes that provided significant experimental evidence of the cooling modes effects on the purity of TTCP. Phase transformations of starting materials at high temperatures were characterized by (Thermo Gravimetric Analysis-Differential Scanning Calorimetry) TGA–DSC, XRD and FTIR analysis.

Farzadi *et al.* [18] studied and investigated synthesis of HA/β-TCP nanocomposite by microwave synthesis method for comparison with the conventional wet chemical methods. The chemical and phase composition, morphology and particle size of powders were characterized by FTIR, XRD and Scanning Electron Microscopy (SEM), respectively. The use of microwave irradiation resulted in improved crystallinity. The amount of HA phase in BCP composite ranged from 5 % to 17 %. The assessment of bioactivity was done by soaking of powder compacts in simulated body fluid (SBF). The decrease in pH of the solution in the presence of β-TCP indicated its biodegradable behavior. Rod-like HA particles were newly formed during the treatment in SBF for microwave assisted substrate synthesis. In contrast, globular particles precipitate under same conditions if BCP substrates were synthesized using conventional wet chemical methods

Raynaud *et al*. [19] synthesized HA using wet method. The purpose of this work was synthesis HA by various molar ratio of Ca/P between 1.50 to 1.667. The thermal stability of powders is also investigated to precise the structural changes and stability domains of the different phases. Single phased apatite calcium phosphate powders $Ca_{10-x}(PO_4)_{6-x}(HPO_4)_x(OH)_{2-x}$ with Ca/P molar ratio ranging from 1.5 to 1.667 ($0 \leq x \leq 1$) were synthesized using wet method. Outside this compositional range the powders were biphasic mixtures composed of a calcium phosphate apatite and $CaHPO_4$ (Ca/P < 1.5) or $Ca(OH)_2$ (Ca/P > 1.667). Temperature and pH of synthesis were the preponderant parameters for the control of the precipitate composition. The precision of the chemical composition requires the use of several perfect techniques and heat treatment of powder. These techniques include high resolution and high

temperature X-ray diffractometry and FTIR and show that very small variations of the Ca/P molar ratio of the powder lead to great changes in powder composition and characteristics after thermal treatment.

Sargin *et al*. [20] synthesized $Ca_4P_2O_9$ (TTCP), a major compound of a cement, in dentistry through different solid-state reactions, at 1300 and 1350°C. Modified methods were used for the reported reactions and a new method of synthesis was suggested, which was given by the following equation:

$$4CaCO_3 + 2NH_4H_2PO_4 \rightarrow Ca_4P_2O_9 + 4CO_2 + 2NH_3 + 3H_2O$$

The refined monoclinic parameters of TTCP were found to be a = 7.017(4), b = 12.021(8), c = 9.483(6) A° and β = 88.21(8)°, which are in good agreement with the reported data. The space group is $P2_1/m$. The IR spectrum of TTCP was analyzed with respect to space group $P2_1$ /m and the band assignments were done for the first time in this work.

Laurent and Didier. [21] studied the osseointegration of two porous calcium phosphate ceramics (HA and β-TCP) with four different pore size ranges. This study was performed to quantify the bone ingrowth and biodegradability of the ceramic according to their pore size ranges (45 - 80 μm, 80 - 140 μm, 140 - 200 μm, and 200 - 250 μm). HA and β-TCP cylinders were implanted into the femoral condyles of rabbits and were left in situ for up to 12 months. Bone ingrowth occurred at a higher rate into the TCP than into the HA ceramics with the same pore size ranges. The amount of newly formed bone was statistically smaller ($p < 0.05$) into ceramics with 45 - 80 μm pore size than with larger pore size, whatever the implantation time for HA and until four months for TCP. No statistical difference was noted between the three highest pore size ranges. No implant degradation was noted up to four months. Their results suggest that a pore size larger than 80 μm improves bone ingrowth in both HA and TCP ceramics. Bone formation was higher rate within the TCP implants than within the HA implants.

Driessens *et al*. [22] fabricated sintered microporous cylinders of HA, β-TCP and rhenanite ($CaNaPO_4$) implanted in the bone of the forehead of the domestic pig (Sus scrofa). Implants together with the surrounding bone were retrieved after 6 and 12 weeks. XRD showed that HA and β-TCP maintain their crystal structure upon implantation. However, rhenanite is transformed completely into an apatite within 6 weeks, which later incorporates sodium and carbonate. Both β-TCP and rhenanite implants showed some resorption but were otherwise covered with new bone. Electron microprobe analysis showed that the mineral at the interface had a Ca/P mole ratio characteristic of new bone. It shown that a certain distance from the interface lower Ca/P mole ratios, characteristic of precursor phases of bone mineral. This suggests that the deposition of new bone starts, at least partially, from the surface of the implant. Therefore, β-TCP as well as rhenanite may be called an osteoconductive biomaterial.

Brandt *et al*. [23] studied the resorption and osteointegration of the nanocrystalline hydroxyapatite Ostim® in a rabbit model. The material was implanted either alone or in combination with autogenic or allogenic bone, into the distal rabbit femora. After a survival time of 2, 4, 6, 8 and 12 weeks the implants had been evaluated using light and electron microscopy. They observed a direct bone contact as well as inclusion into soft tissue. But they could observe only marginal decay and no remarkable resorption in the vast majority of implants. In situ the nanocrystalline material mostly formed densely packed agglomerates, which were preserved once included in bone or connective tissue. A serious side effect was the initiation of osteolysis in the femora far from the implantation site, causing extended defects in the cortical bone.

Benhayoune *et al*. [24] implanted dense pure HA-ceramic cylinders into cortical sheep femurs for periods ranging from 2 weeks to 18 months. The samples were then sectioned and examined using back-scattered and secondary SEM, and the interface was analyzed using Energy Dispersive Spectrometry (EDS). A histomorphometry measurement was also performed using an image analysis device coupled to a light microscope. It appeared that after three weeks the cylinders were in direct contact

with immature bone, and the bone maturated within three months. The implant surface showed moderate signs of resorption and some grains were released from the surface. The resorption zone was only a few micrometers thick after 18 months. The bulk ceramic contained default zones of increased porosity. They can constitute a fragile zone when located close to the surface in which the resorption rate is increased. They conclude that dense pure HA is poorly degraded when implanted in the cortical bone. Degradation depends on the defaults found on the ceramic structure and the remodeling of the bone surrounding the material.

Punyanitya *et al*. [25] provided a ceramic block from bovine bone-bioglass composite was implanted in the subcutaneous tissue at the back of rat necks to study biocompatibility. The other specimen grains were implanted into the bone marrow cavity of rabbit femurs. From pathological examination of the soft tissue around the implantation, there were no signs of intense inflammation or adverse side effect on the rats and rabbits. For implantations in the rabbit femur cavities, the results showed new bone growth from the host bone to the specimens, about 30% by volume after 1 month, and 70% after 6 months.

1.3 Principles, Models, Rationale or Hypothesis

Hydroxyapatite ($Ca_{10}(PO_4)_6(OH)_2$, (HA)) is one of the most effective biocompatible materials and it is found to be the major component of bone. It is widely used in biological materials due to the apatite-like structure of enamel, dentin and bones, known as “hard tissue” [26]. The stoichiometric crystal structure of HA has a monoclinic system with P21/b as its space group [27]. However, at temperatures above ~250°C, there is a monoclinic to hexagonal phase transition in the HA (space group $P6_3/m$) [28]. It is interpreted in terms of the aggregation of $Ca_9(PO_4)_6$ clusters, the so-called Posner’s clusters, that have been widely used since the publication of an article by Posner and Betts [29]. The $Ca_9(PO_4)_6$ clusters appeared to be energetically favored in comparison to alternative candidates, including $Ca_3(PO_4)_2$ and $Ca_6(PO_4)_4$ clusters [30]. In hexagonal HA, the hydroxide ions are more disordered within each

row when compared with the monoclinic form, pointing either upwards or downwards in the structure. This induces strains that are compensated for by substitutions or ion vacancies. Some impurities, like partial substitution of hydroxides by fluoride or chloride, stabilize the hexagonal structure of HA at ambient temperatures. For this reason, hexagonal HA is seldom the stoichiometric phase, and it is very rare that single crystals of natural HA exhibit the hexagonal space group. A shell model was developed to study the lattice dynamics of HA, while a cluster growth model was created to illustrate its growth [31]. Polarization characteristics [32] and pyroelectrical properties [33] of HA bioceramics have been investigated. First-principle calculations for the elastic properties of doped HA and vacancy formation in HA were performed. From above mentioned, some ions such as HPO_4^{2-}, CO_3^{2-} and F^{-1} replace partial PO_4^{3-} and OH^{-1}. Some other earth elements such as Mg^{2+} and Sr^{2+} can replace Ca^{2+}. The common formula should be $Ca_{10-x+y}(PO_4)_{6-x}(OH)_{2-x-2y}$, where $0 < x < 2$ and $0 < y < x/2$. For instance, the bone composition can be represented by the formula of $Ca_{8.3}(PO_4)_{4.3}(HPO_4,CO_3)_{1.7}(OH,CO_3)_{0.3}$ [34-36]. In a physiological environment, bone is a non-stoichiometric HA of calcium and phosphorus molar ratio from 1.5 to 1.67 which dependent on the age and bone site in human. Basic science of HA was studied from the XRD and FTIR. These techniques to study HA sintered at different temperatures and reported that after sintering at 900°C. The material was fully hydroxylated after sintering at higher than 900°C and then dehydroxylation occurred. Dehydration of HA was produced by processes such as high temperature solid state reaction, result in the formation of oxyhydroxyapatite: $Ca_{10}(PO_4)_6(OH)_{2-2x}O_xV_x$ (where V is a hydroxyl vacancy). HA has a $P6_3/m$ space group: This indicates that the lattice is primitive Bravais. There is a six fold axis parallel to the c axis and a 1/2 (3/6) translation along the length of the c axis (a screw axis) with a mirror plane situated perpendicular to the screw axis and the c axis. Parameter of a and c value for HA are 0.9418 nm and 0.6884 nm, respectively [37]. The structure assumed by any solid is such that, on an atomic level, the configuration of the constituents is of the lowest possible energy. In phosphates, this energy requirement results in the formation of discrete subunits within the structure and the PO_4^{3-} group forms a regular

tetrahedron with a central P^{5+} ions and O^{2-} ions at the four corners. In a similar manner, the $(OH)^-$ groups are also ionically bonded. In terms of the volume occupied, the oxygen ions exceed all other elements in phosphates. Any other elements present may therefore be considered as filling the interstices, with the exact position being determined by atomic radius and charge [38, 39] (**Figure 1**).

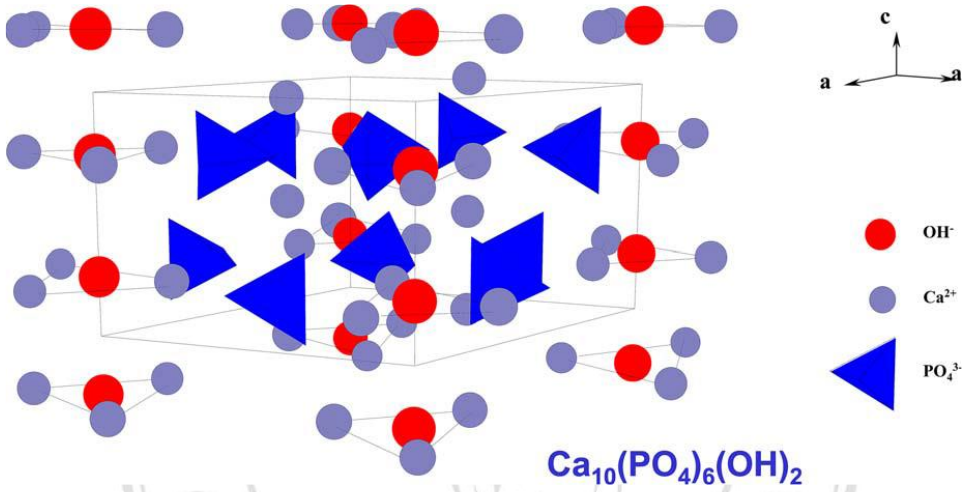

Figure 1 HA structure projected down the c-axis on the basal plane [38].

The HA lattice contains two kinds of calcium positions; columnar and hexagonal. There is a net total of four "columnar calcium" ions that occupy the [1/3, 2/3, 0] and [1/3, 2/3, 1/2] lattice points. The "hexagonal calcium" ions are located on planes parallel to the basal plane at c = 1/4 and c = 3/4 and the six PO_4^{3-} tetrahedral are also located on these planes. The $(OH)^-$ groups are located in columns parallel to the c axis. At the corners of the unit cell, this may be viewed as passing through the centers of the triangles formed by the "hexagonal calcium" ions. Successive hexagonal calcium triangles are rotated through 60° [40] (**Figure 2**).

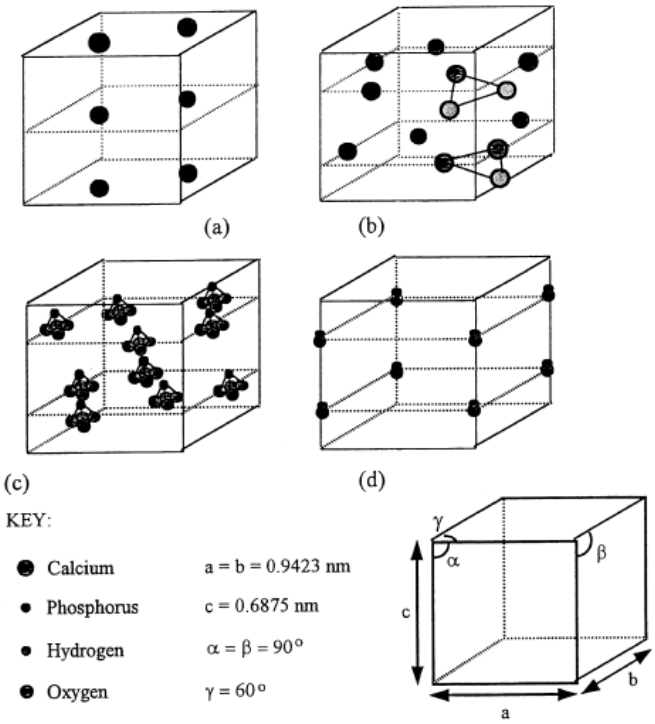

Figure 2 Theoretical positions of the ionic species within the unit cell of HA [39].

Defects and impurities in HA may be identified as either substitutional or distinct, external crystalline phases. Ions that may be incorporated into the HA structure, either deliberately or undeliberately, include carbonate ions (substituting for hydroxyl or phosphate groups), fluoride ions (substituting for hydroxyl groups), silicon, or silicate ions (substituting for phosphorus or phosphate groups) and magnesium ions substituting for calcium [41-44].

There are two sources of apatite mineral: the first one from biological and the other from mineral deposits such as phosphate rock or phosphorite. A sedimentary rock is the essential mineral component which is carbonate fluoroapatite [45]. HA can be prepared by several synthetic routes including solid state reactions [46], chemical precipitation [47], hydrothermal reactions [48], sol-gel methods [49] and mechanochemical methods [50] by using different calcium and phosphorus containing initial materials. Nowadays, there are several methods to obtain synthetic HA. This research used solid precursors for synthesis. The production of HA by the ceramic method is a traditional laboratory process, which can be carried out using different

precursor salts from the phosphate and carbonate families, respectively. The traditional methods for the consolidation of ceramic powders are used dry state. This method call that the microstructure of the green body. Method has a significant effect on the subsequent firing stage. If violent variations in packing density occur in the green body, the fired body will contain heterogeneities that will limit the engineering properties. The homogeneous packing of particles in the green body is the desired goal of the consolidation step. Since the packing density controls the amount of shrinkage during firing, the achievement of high packing density is also desirable. Geometrical particle packing concepts provide a useful basis for understanding how the structure of the consolidated powder. An important practical consideration is the extent to which the parameters of the consolidation process can be control the packing uniformity and packing density of the green body [51].

1.3.1 Mechanism of solid-state sintering

Sintering is a process that provided the powder to join together and reduces the porosity of the body. It is required in the fabrication process. The process can reduce surface area, bulk volume reduction (densification), grain growth, and improve mechanical properties. This is an integration of temperature, time, and ceramic precursor which develops the process into a coherent microstructure [52]. Sintering takes place is three fundamental stages: an initial stage, an intermediate stage, and a final stage. The distinction between initial and intermediate stage sintering is rather vague. For the fine powder, which has the lower density initially, sinters to a higher density at a lower temperature because it has a higher specific surface area. In the simplest form, the driving force for sintering is the reduction of the surface energy of a powder compact by the replacement of solid-air interface with lower energy solid-solid interfaces. As an order of magnitude estimate, the net decrease in free energy for a 1 μm of particles size material is about 1 cal/gm [53]. This driving force for sintering is small and should not be squandered on mechanisms (such as surface diffusion and evaporation-condensation) that do not lead to densification.

Figure 3 The initial, intermediate and final stages of sintering [54].

In **Figure 3**, the initial, intermediate and final stages of sintering. The various stages of sintering composed of initial Stage: 1. Particle surface smoothing and rounding of pores 2. Grain boundaries form 3. Neck formation and growth 4. Homogenization of segregated material by diffusion 5. Open pores 6. Small porosity decreases < 12%. Intermediate Stage: 1. Intersection of grain boundaries 2. Shrinkage of open pores 3. Porosity decreases substantially 4. Slow grain growth (Differential pore shrinkage and grain growth in heterogeneous material) Final Stage: 1. Closed pores-density > 92% 2. Closed pores intersect grain boundaries 3. Pores shrink to a limiting size or disappear 4. Pores larger than the grains shrink very slowly [53].

These stages are the typical progression of events that take place during sintering. However, sometimes the density does not increase even though the pores change shape. This is called coarsening. The difference between sintering and coarsening is schematically shown in **Figure 4**. If the inter particle separation distance remains the same, coarsening takes place. If the inter particle separation distance decreases, sintering takes place. Only sintering leads to an increase in density, which is referred to as densification. Almost all density variations in the green compacts tend to be amplified during sintering. These density variations lead to warping and cracking during sintering. For this reason, we have devoted an enormous effort in the preceding chapters to the subject of density uniformity in the ceramic green body. Rejecting the ceramic part after sintering is tantamount to throwing away the raw material as well as all the energy and labor used to make the part. Its rejection at this stage is a very expensive loss. In some cases, the rejection rate can be as high as 50% [53].

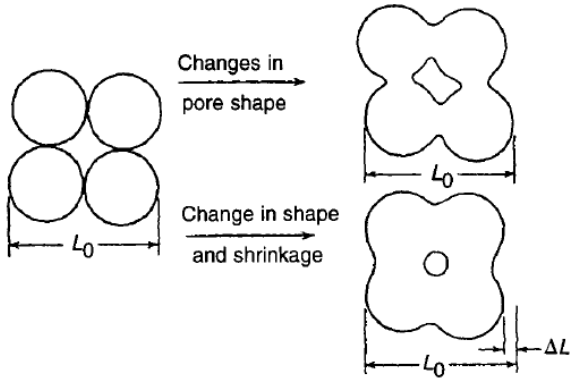

Figure 4 The differences between coarsening and sintering [53].

Some cases can the faulty sintered ceramic part be recycled by grinding as raw material. This grinding incurs yet a higher energy cost for this raw material but this may be cheaper than buying fresh raw materials.

After burnout of the binder, we are left with a green body that is composed of ceramic particles in contact as shown in **Figure 4**. As the temperature is increased, material flows from various sources within the ceramic green body to the neck at the intersection between particles, as shown in **Figure 5** [55]. This neck has a negative curvature, compared to the positive curvature of the spherical ceramic particle, and results in a energetically more favorable location for the material. These pathways are drawn on **Figure 5** and consist of surface, lattice and grain boundary diffusion, as well as vapor phase diffusion. These pathways give rise to different mechanisms of sintering.

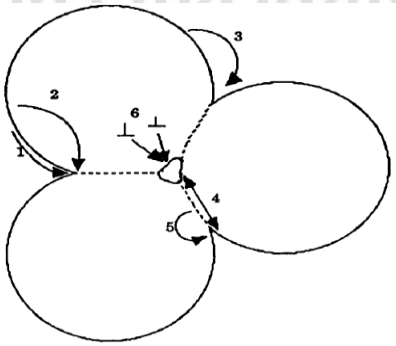

Figure 5 Pathways for the transport of material during the initial stage of sintering [55].

The interparticle bonding is not complete, so further sintering is required. Depending on the material system, this sintering will take place by liquid phase or solid state sintering. Previously, solid state sintering was discussed. The sintering kinetics depends upon the rate determining step, which can be viscous flow, grain boundary diffusion or lattice diffusion. The sintering kinetics involved with heating schedule, which have a more complex temperature and time relationship, as in the sintering of ceramics for industrial applications. A general heating schedule is composed of 6 stages [56] (**Figure 6)**.

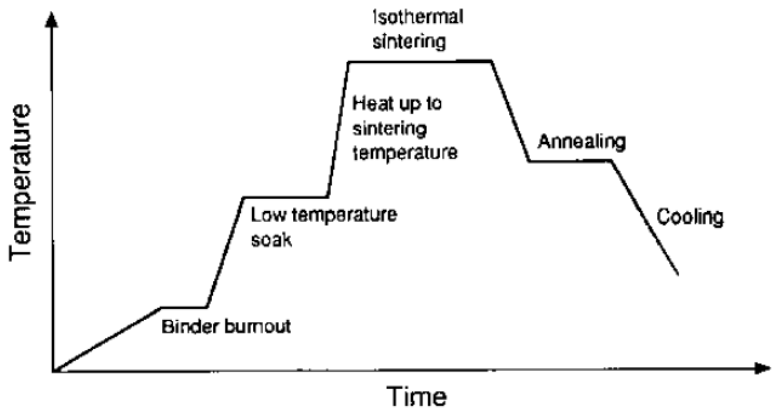

Figure 6 Pattern of a general heating schedule [56].

Stage 1. Binder burnout indicated removal of volatile materials such as adsorbed water, and the conversion of additives such as metal organic compounds or organic binders take place. The heating rate is often slow and rate often < 2°C/min, since rapid heating may cause boiling and evaporation of organic additives, leading to swelling and even cracking of the specimen. Typically, the hold temperature in this stage is, at most, 400–500°C.

Stage 2. Low-temperature soak included to promote chemical homogenization or the reaction of powder components. The hold temperature is commonly below that for the onset of measurable sintering. Chemical homogenization may, for example, involve a solid-state reaction in which a small amount of doped is incorporated into the powder or a reaction leading to the formation of a liquid phase.

Stage 3. Heat-up to the sintering temperature involves heat-up to the isothermal sintering temperature. The heating rate is limited by the sample size and the thermal characteristics of the furnace. For large bodies, the heat-up times can stretch for many hours to avoid temperature gradients that could lead to cracking or to avoid the formation of a dense outer layer on an incompletely made more dense of core, as would result from differential densification. In laboratory-scale experiments with small specimens, it is often observed that a faster heating rate in this stage enhances the densification in the subsequent isothermal sintering stage. A possible explanation of this observation is that the coarsening of the powder during the heat-up is reduced due to the shorter time taken to reach the isothermal sintering temperature, thereby resulting in finer microstructure at the start of isothermal sintering.

Stage 4. Isothermal sintering is chosen to be as low as possible yet compatible with the requirement that densification be achieved within a reasonable time (typically less than 24 h). Higher sintering temperatures lead to faster densification, but the rate of coarsening also increases. The increased coarsening rate may lead to abnormal grain growth where pores are trapped inside large grains. Whereas densification proceeds faster, the final density may be limited.

Stage 5. Annealing included prior to final cool-down of the material to relieve thermal stresses, to allow for precipitation of second phases, or to modify the chemical composition or the microstructure. Annealing to reduce thermal stresses is common in systems that contain a glassy matrix or that undergo a crystallographic transformation involving a volume change. Modification of the chemical composition and the microstructure is common in many functional ceramics such as ferrites.

Stage 6. Cool down to room temperature refer to prevent large temperature gradients that can lead to cracking, when compositional or microstructure modification must be achieved, the cooling rate needs to be carefully controlled. The cooling rate can influence the precipitation of second phases and their distribution in the fabricated.

1.3.2 Phase diagram of $CaO-P_2O_5$ in a water atmosphere [57]

Thermodynamic stability of the various calcium phosphates is summarized in the form of the phase diagram shown in **Figure 7**. The binary equilibrium phase diagram between CaO and P_2O_5 gives an indication of the compounds formed between two oxides. It is possible to identify the naturally occurring calcium phosphate minerals. This figure shows the phase diagram of CaO and P_2O_5 at 500 mm Hg partial pressure of water. A phase diagram show the stable phase of HA below 1360°C, and decomposed into TTCP ($Ca_4(PO_4)_2O$) and alfa-TCP (α-$Ca_3(PO_4)_2$) above 1360°C. The complete decomposition occurs at 1550 to 1570°C, and HA becomes the mixture of liquid, TTCP and α-TCP above 1570°C. Without water vapor, HA starts loss of OH group at even as low as 900°C.

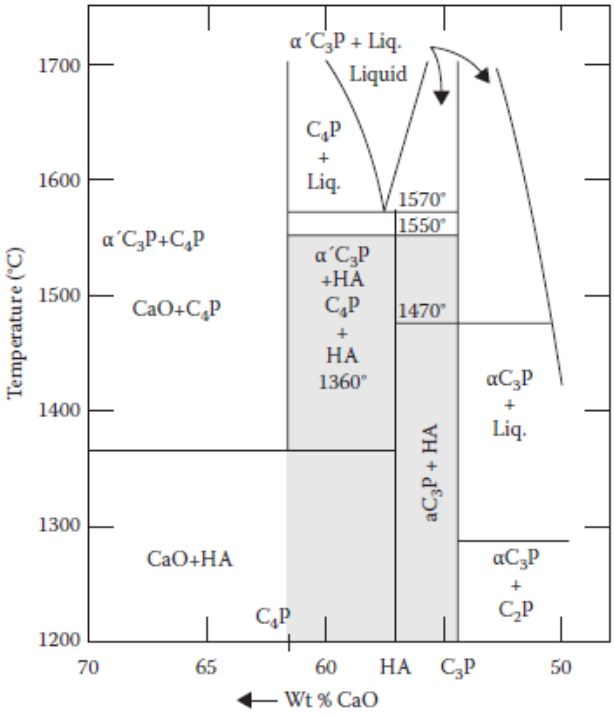

Figure 7 Phase diagram of $CaO–P_2O_5$ [57].

The decomposition has significant above 1000°C in air, N_2 or Ar. For sintering, the preferred temperatures lower 1360°C under at least 500 mm Hg water-vapor pressure.

Shaded area is processing range to yield HA. The diagram does not indicate the phase boundaries of apatite due to the absence of hydroxyl groups [57]. For plasma thermal spray at temperature above 5000°C and the decomposition occur certain. The final phase composition of HA coating contains crystalline HA, amorphous phase, TTCP, α-TCP, β-TCP and CaO. However, from the binary diagram an indication may be obtained of the stability of other calcium phosphates with various temperatures [58].

Calcium carbonate ($CaCO_3$) is a raw material made from limestone. It is non-toxic, white and bright color. Therefore it is very useful in a variety of situation such as for a filler and extender for the paper industry, paint industry, plastics industry, PVC, and rubber industry. It is also used as an ingredient in toothpaste, detergents and pharmaceutical drugs. Moreover, it is also used in the manufacture (parts and accessories), such as computer, telephone, phone cover line, insulator of electrical cables, eraser, glove and glasses [59].

Calcium is a necessary mineral that is ranked as the fifth highest volume in the human body about 90 percent of calcium being used to build bones and teeth. Calcium sends signals through the nerves that control the muscles and other organs. It is an important key in the mechanism of blood clotting, produces energy in the body, prevents cramps in pregnant women, and prevents colon cancer etc., Therefore, it can be seen that calcium is very important for the human body, especially for menopausal women and the elderly [59].

The PO_4^{3-} -group in the apatite-group minerals can be replaced by a variety of other tetrahedral anion groups (e.g., AsO_4^{3-}, VO_4^{3-}, MnO_4^{3-}, CrO_4^{3-}, SO_4^{2-}, SeO_4^{2-}, CrO_4^{2-}, BeF_4^{2-}, SiO_4^{4-}, GeO_4^{4-}, SbO_3F^{4-}, SiO_3N^{5-}, and BO_4^{5-}). Another tetrahedral anion group is replaced for PO_4^{3-} is $(OH)_4^{4-}$ by analoging to that in "hydrogarnets". But there is still no structural evidence for the $(OH)_4^{4-}$ group has been found in the apatite-group minerals or their synthetic analogs. Other polyhedral groups that have been shown to substitute for PO_4^{3-} in the apatite-group minerals include CO_3^{2-}, BO_3^{3-} and ReO_5^{3-} end the proposed mechanisms for the replacement of the PO_4^{3-} group in the apatite-group minerals [60, 61].

1.3.3 Biological properties

The principle of in vivo assessment of tissue compatibility of a biomaterial, prosthesis, or medical device is to determine the biocompatibility or safety of the biomaterial, prosthesis, or medical device in a biological environment. Biocompatibility has been defined as the ability of a medical device to perform with an appropriate host response in a specific application, and biocompatibility assessment is considered to be a measurement of the magnitude and duration of the adverse alterations in homeostatic mechanisms that determine the host response. The term “medical device” will be used to describe biomaterials, prostheses, artificial organs, and other medical devices, and the terms “tissue compatibility assessment”, “biocompatibility assessment” and “safety assessment” will be considered to be synonymous. From a practical perspective, the in vivo assessment of tissue compatibility of medical devices is carried out to determine that the device performs as intended and presents no significant harm to the patient or user. Thus, the goal of the in vivo assessment of tissue compatibility is to predict whether a medical device presents potential harm to the patient or user by evaluations under conditions simulating clinical use [62]. In the selection of biomaterials to be used in device design and manufacture, the first consideration should be fitness for purpose with regard to characteristics and properties of the biomaterials. These include chemical, toxicological, physical, electrical, morphological, and mechanical properties. Relevant to the overall in vivo assessment of tissue compatibility of a biomaterial or device is knowledge of the chemical composition of the materials, including the conditions of tissue exposure as well as the nature, degree, frequency, and duration of exposure of the device and its constituents to the intended tissues in which it will be utilized.

For the short term implantation evaluation out to 12 weeks, mice, rats, guinea pigs, or rabbits are the usual animals utilized in these studies. For the longer term testing in subcutaneous tissue, muscle, or bone, animals such as rats, guinea pigs, rabbits, dogs, sheep, goats, pigs, and other animals with relatively long life expectancy are suitable. If a complete medical device is to be evaluated, larger species

may be utilized so that human-sized devices may be used in the site of intended application. For example, substitute heart valves are usually tested as heart valve replacements in sheep, whereas calves are usually the animal of choice for ventricular assist devices and total artificial hearts [62, 63].

In developing materials used for implantation consideration must be given to both the influence of the implanted material on the body and how the body affects the integrity of the material. The body will treat implants as inert, bioactive, or resorbable materials. Generally "inert" materials will evoke a physiological response to form a fibrous capsule, thus, isolating material from the body. HA is grouped into the category of bioactive and resorbable materials. A bioactive material will dissolve slightly but promote the formation of an apatite layer before interfacing directly with the tissue at the atomic level. Such an implant will provide good stabilization for materials that are subject to mechanical loading. A bioresorbable material will dissolve and allow tissue to grow into any surface irregularities but it may not necessarily interface directly with the material [64]. The route and conditions under which synthetic HA is produced will greatly influence its physical and chemical characteristics. Factors that affect the rate of resorption of the implant include physical factors such as the physical features of the material (e.g., surface area, crystallite size), chemical factors such as atomic and ionic substitutions in the lattice, and biological factors such as the types of cells surrounding the implant and location, age, species, sex and hormone levels. For biological assays, tissue reaction to HA for surgical implants evaluated the effects of the materials on animal tissue in which it is implanted. The experimental protocol is designed to provide assessment of the systemic toxicity, immune response, carcinogenicity, teratogenicity or mutagenicity of the materials. It applies only to materials with projected applications in humans where the materials will reside in bone or soft tissue in excess of 30 days and will remain unabsorbed [65].

1.4 Objectives of this thesis

1.4.1 To study the mechanism of the sintering reaction for synthesis of HA.

1.4.2 To study the optimization condition of final product for producing synthetic HA.

1.4.3 To study biological properties of the HA ceramics by animal testing.

1.5 Scope and Study

The scope of my research is the study the reaction of a solid-state diffusion mechanism using the sintering method. The starting materials were obtained from calcium carbonate ($CaCO_3$) powder (analytical grade, Ajax, Netherland), and ammonium dihydrogen phosphate ($NH_4H_2PO_4$) powder (analytical grade, Merck, Germany). Characterizations and to studies of their chemical, physical and mechanical properties are controlled by three parameters, such as chemical composition, sintering temperature and soaking time. To study a quantitative X-ray diffraction analysis will indicate HA content of sample when compare with standard HA for surgical implants. All parameters for synthesis are covers material requirements for synthetic HA and animal testing in soft tissue of laboratory rats [65, 66].